Spring 5-1-2013

Biophysical Characterization of Optimized Self-Assembling Protein Nanoparticles as a Malaria Vaccine

Sophia Walker
University of Connecticut - Storrs, sophia@myusdomain.com

Biophysical characterization of optimized self-assembling protein nanoparticles as a malaria vaccine

Honors Thesis

Sophia Walker

Structural Biology/Biophysics

Research Advisor: Peter Burkhard, Ph.D.

Honors Advisor: James Cole, Ph.D.

Spring 2013

Table of Contents

Acknowledgements 3

Abbreviations 4

Figures 5

Abstract 6

Introduction 7

Materials and Methods 12

Results 17

Discussion 29

References 31

Acknowledgements

I would like to thank Dr. Peter Burkhard, my research advisor, for taking me into his lab, and for his continued guidance and support throughout my undergraduate studies. I thank Dr. James Cole, my honors advisor, for offering constructive input on my thesis and my undergraduate coursework. I wish to thank Dr. Sharareh Emadi for teaching me all of the laboratory and analytical skills necessary to complete this thesis, and for her invaluable advice and encouragement throughout this project. I would like to thank Dr. Tais Doll for introducing me to the basics of research and laboratory work. Lastly, I thank all of the members of the Burkhard Lab, past and present, for fostering such a collaborative and enjoyable research environment. Your contributions to my education will always be remembered and much appreciated.

Abbreviations

BCA Assay: Bicinchoninic acid assay

CSP: Circumsporozoite Protein

DLS: Dynamic Light Scattering

E. coli: *Escherichia coli*

EM or TEM: Transmission Electron Microscopy

F5c: Pandora F5c

F5de: Pandora F5de

FPLC: Fast Protein Liquid Chromatography

Hepes: 4-(2-hydroxyethyl)-1-piperazineethanesulfonic acid

His-tag: Histidine tag

HIV: Human Immunodeficiency Virus

IPTG: Isopropyl β-D-1-thiogalactopyranoside

LB: Luria-Bertani Broth or Medium

Mes: 2-(*N*-morpholino)ethanesulfonic acid

Ni-NTA: Nickel-nitrilotriacetic acid

OD: Optical Density

PCR: Polymerase Chain Reaction

SAPN: Self-Assembling Protein Nanoparticle

SARS: Severe Acute Respiratory Syndrome

SDS-PAGE: Sodium Dodecyl Sulfate Polyacrylamide Gel Electrophoresis

SOC: Super Optimal Broth with Catabolite Repression Medium

Tris: Tris(hydroxymethyl)aminomethane

Figures

Figure 1: Monomeric Unit of the Nanoparticle

Figure 2: Most Recent Construct

Figure 3: Modified Constructs

Figure 4: Purification Profile

Figure 5: Fraction Contents

Figure 6: Quick Refolding

Figure 7: Protein Concentration Determination

Figure 8: Direct Refolding

Figure 9: Stability Testing in Hepes Buffer

Figure 10: Stability Testing in Tris Buffer

Figure 11: Stability Testing at Different Temperatures in Tris Buffer

Figure 12: TEM Images of Pandora F5de in Tris Buffer

Figure 13: Pandora F5de in Hepes Buffer

Abstract

Malaria is an infectious disease that affects several million individuals worldwide and is a significant international public health issue. While there is currently a malaria vaccine in phase III clinical trials, recent results demonstrate that it is only about 35% effective in reducing the incidence of the disease [2]. The use of self-assembling protein nanoparticles (SAPNs) that display epitopes of the repeat sequence of the circumsporozoite protein of *Plasmodium falciparum*, the parasite that causes malaria, has been shown to elicit a strong immune response. This prototype has potential for further improvement by altering the epitope regions of the nanoparticles to be more compatible with humans and by modifying the nanoparticle backbone to be more soluble and compact. It was predicted and demonstrated, through dynamic light scattering and transmission electron microscopy imaging, that these slight changes to the nanoparticle construct could result in increased stability and immunogenicity for this promising malaria vaccine.

Introduction

Malaria is an infectious disease that affects several million individuals worldwide. According to the World Health Organization, malaria is endemic in more than 100 countries and resulted in approximately 660,000 deaths in 2010 [1], making this disease a significant international public health issue. While there is currently a malaria vaccine in phase III clinical trials, recent results demonstrate that it is only about 35% effective in reducing the incidence of the disease [2]. The use of self-assembling protein nanoparticles (SAPNs) that display epitopes of the repeat sequence of the circumsporozoite protein (CSP) of *Plasmodium falciparum*, the parasite that causes malaria, have been shown to elicit a strong immune response. This prototype has potential for further improvement by altering the epitope regions of the nanoparticles to be more compatible with humans and by modifying the nanoparticle backbone (trimeric and pentameric coiled-coils) to be more soluble and compact. It is predicted that these slight changes to the nanoparticle construct could result in increased stability and immunogenicity for this potential malaria vaccine.

SAPNs are small proteins that assemble to form oligomers with diameters on the nanoscale. Studying particles on the nanoscale has become exceptionally relevant in recent years, especially in the area of rational drug design and vaccine development. This particular nanoparticle design (figure 1A), which has proven effective for the potential development of SARS and HIV vaccines [3, 4], involves the formation of an oligomer with icosahedral symmetry (i.e. 20 planes with 2, 3, and 5 fold symmetry axes [5]) from sixty self-associating identical protein monomers [6]. Each monomer contains a sequence that forms a pentameric and trimeric coiled-coil backbone (figure 1B), connected by a one to two amino acid linker [6]. Importantly, these fully assembled nanoparticles have a general appeal in the area of vaccine

design, as their diameter is often on the same order as many viruses [5, 7]. Antigenic peptide sequences, which, in this case originate from the *Plasmodium falciparum* sporozoite, can be attached to each end of the backbone. These nanoparticles assemble into large globular oligomers with many copies of the epitope exposed on the surface. Thus, such a design allows for multiple opportunities for antigen presentation that could ultimately result in more significant and longer lasting levels of immunity in the host organism.

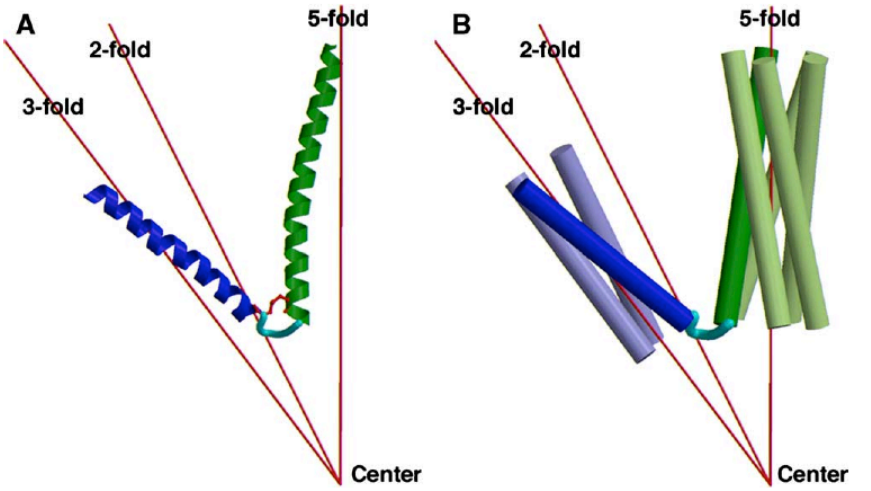

Figure 1. Monomeric Unit of the Nanoparticle. (A) The peptide monomer with the trimer at the c-terminal end in blue and the pentamer at the n-terminus in green. (B) These monomers assemble into coiled coils, shown as cylinders, along the three-fold and five-fold axes of symmetry. The red lines indicate the axes of symmetry. The formation of the complete icosahedron shape requires the association of 60 monomers in solution. Image taken from [6].

To date, the most current SAPN vaccine prototype for malaria, known as PfCSP-KMY-SAPN (figure 2A, B), exhibits three $CD8^+$ T cell epitopes from CSP from *Plasmodium falciparum* attached at the pentamer region of the protein and the universal CD4 T-helper cell epitope incorporated into the trimer domain [8]. Also, attached to the C-terminal end of the trimeric domain is the B-cell epitope ($NANP_4$) from the repeat region of the CSP [8]. Thus, this design has the capability of activating both humoral and cell-mediated immunity. Each protein monomer also has a histidine tag at the pentameric, N-terminal end so that it can be purified

easily. This nanoparticle design with epitopes specific to mice (from *Plasmodium berghei* and *Plasmodium vivax*), has been shown to result in a protective immune response by T-cell and B-cell proliferation especially in the liver and blood in Balb/c and related strains of mice [8]. This study thus demonstrated that this particular SAPN design containing the CSP epitopes could result in a protective immune response. Importantly, the vaccine formulation was administered to the mice without addition of an adjuvant, demonstrating that the nanoparticles are capable of eliciting an effective immune response without additional, supplementary stimulation of the immune system. In this malaria vaccine design, and in others, the epitopes from CSP are incorporated because CSP is especially relevant to the infection process of the host. CSP is present on the surface of the sporozoites [9] that enter and infect the host upon being bitten by a mosquito carrier and is a significant component in the infection process of the liver [9]. In this particular vaccine design, the repeat region of CSP was incorporated into the protein monomer of the self-assembled nanoparticle.

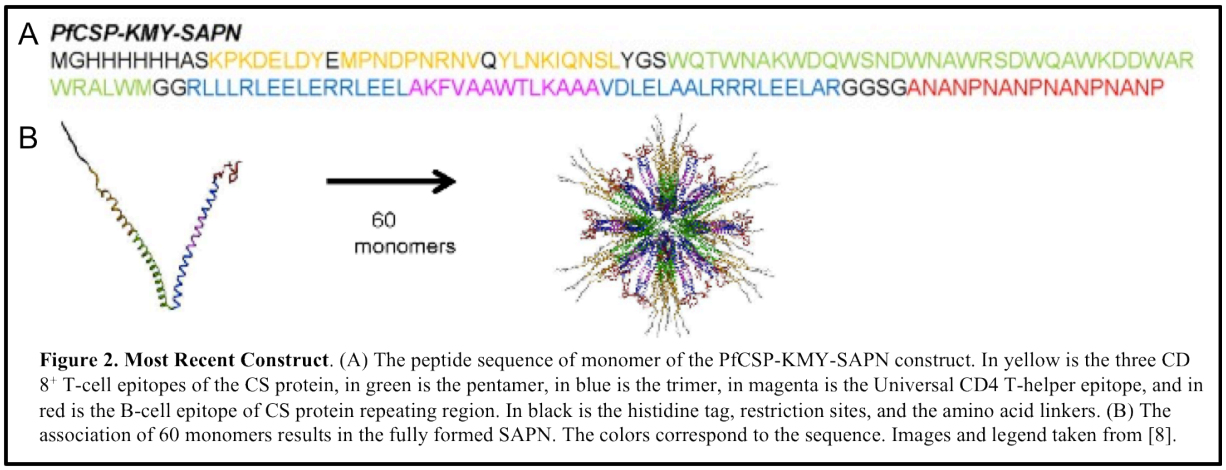

Figure 2. Most Recent Construct. (A) The peptide sequence of monomer of the PfCSP-KMY-SAPN construct. In yellow is the three CD 8^+ T-cell epitopes of the CS protein, in green is the pentamer, in blue is the trimer, in magenta is the Universal CD4 T-helper epitope, and in red is the B-cell epitope of CS protein repeating region. In black is the histidine tag, restriction sites, and the amino acid linkers. (B) The association of 60 monomers results in the fully formed SAPN. The colors correspond to the sequence. Images and legend taken from [8].

Because the PfCSP-KMY-SAPN prototype exhibiting the *Plasmodium falciparum* (human malaria strain) CSP $CD8^+$ epitopes can elicit an effective immune response in mice, some modifications have been made to this design so that it can be further modified for humans. In this new design, referred to as Pandora F5c (figure 3A), and additional fourth $CD8^+$ epitope of

CSP has been incorporated in the trimeric region along with a new universal $CD4^+$ helper T-cell domain (specific to humans) in the trimer. Also, two amino acid replacements in the overall protein trimeric and pentameric backbone were made, in order to achieve even greater solubility, compactness, and stability in solution. The fully modified construct that was purified and characterized herein is referred to as Pandora F5de (figure 3B). In the pentameric region of the protein an arginine (residue 57) was replaced with a glutamic acid, making it more negatively charged. Conversely, a glutamic acid (residue 93) in the trimer was switched with an arginine, resulting in a more positively charged trimeric region. These changes were expected to promote greater attraction between the two regions, so that the assembled nanoparticle would be more compact in solution. Such considerations are exceptionally important as vaccine development continues, due to the nanoparticle design itself, which is highly dependent on the geometric and thermodynamic stability favoring the assembled state [7], and as a result of the requirements associated with vaccine administration and efficacy in future *in vivo* studies [10]. The protein monomer has a molecular weight of about 18 kDa and the correctly assembled SAPN with icosahedral symmetry should be 1083 kDa. Furthermore, the estimated extinction coefficient of the protein is 64, 940 $M^{-1}cm^{-1}$. Based on protein design and modeling methods, the approximate diameter of the fully assembled SAPN is expected to be about 25 nm.

Construct	Sequence
Pandora F5c	MGHHHHHHASKPKDELDYEMPNDPNRNVQYLNKIQNSLYEWNAKWDEWKNDWNDWRRD WQAWKDDWAYWTLTWKYGELYSKLAEIERRVEANERALEELARFVANLSMRLAGLIMVLSF LRNRSADDDPNANPNVDPNANPNANPNANPNK
Pandora F5de	MGHHHHHHASKPKDELDYEMPNDPNRNVQYLNKIQNSLYEWNAKWDEWKNDWNDWRED WQAWKDDWAYWTLTWKYGELYSKLAEIERRVEANRRALEELARFVANLSMRLAGLIMVLSF LRNRSADDDPNANPNVDPNANPNANPNANPNK

Figure 3. Modified Constructs. In orange are the three $CD8^+$ epitopes of *P. falciparum* CS protein in the pentameric region and the fourth in the trimeric region. In green and blue, are the pentameric and trimeric regions, respectively. In Magenta is the Universal CD4 T-helper epitope. Red is the B-cell epitope of the repeat region of *Plasmodium falciparum* CSP. In black is the histidine tag and linkers between regions. Highlighted are the two introduced mutations, R57E and E93R, illustrating the difference between the two constructs.

The modifications, especially the two amino acid replacements of the two backbone modifications, were made and the new protein monomer was expressed in *Escherichia coli*. The protein was purified by affinity chromatography using a His-Trap column, as it historically has resulted in especially pure proteins for similar constructs. Purification was conducted in denaturing conditions (8 M urea), to achieve the greatest purity and to control the refolding conditions once the monomer was purified. The refolding methods, buffer conditions, the general shape, and affects of the applied modifications to the vaccine design described above were evaluated by dynamic light scattering (DLS) and electron microscopy (EM) and compared to the current design. Furthermore, experiments involving buffer effects on the size distribution of the overall assembled nanoparticles and long-term storage at different temperatures were evaluated by DLS. The use of DLS was important, because it allowed for the verification of the approximate diameter of the nanoparticle oligomers, and it demonstrated the presence of any aggregation or other obstacles that could prevent expected assembly of the monomer protein. This is essential for vaccine development with this design, as only the fully assembled particle would be able to elicit an immune response in the host, yet large aggregates would likely result in a negative and undesirable immune response *in vivo*, such as anaphylaxis. EM was used to evaluate the shape and size of the refolded and assembled nanoparticles under the various conditions. It was hypothesized that these modifications to the current construct would improve the malaria vaccine design and advance attempts to evaluate its efficacy in animal models.

Materials and Methods

Introduction of the First (R57E) Mutation. From the existing F5c plasmid, Pandora F5de was prepared by introducing two mutations through PCR-mutagenesis and transformation into DH5α *Escherichia coli* competent cells. PCR-mutagenesis was carried by combining 16 µl of ddH_2O, 2 µl of F5c plasmid (about 100 ng/µl), 0.5 µl of 10 mM dNTP mix, 1.5 µl of 10 uM forward primer (5' TGG ATT GAC TGG CGT CGC GAC TGG CA 3'), 1.5 µl of 10 uM reverse primer (5' CAA CGC TGG CCA GTC TTC ACG CCA GT 3'), 2.5 µl of 10x native *Pfu* buffer, and 1 µl of 2-3 units/µl of *Pfu* DNA polymerase. The dNTP mix, *Pfu* buffer, and native *Pfu* DNA polymerase were acquired from Stratagene and the primers were ordered from Integrated DNA Technologies, Inc. A control without the F5c plasmid was also prepared. PCR was conducted under heating for 5 minutes at 95C, 18 cycles of 30 seconds at 95ºC, 1 minute at 55ºC, and 5 minutes at 72ºC, and lastly 7 minutes at 72ºC. The plasmid was stored at 4ºC. The PCR product was incubated with 1 µl of 20,000 units/ml of Type II restriction enzyme DpnI (acquired from New England BioLabs) for 3 hours at 37ºC. The DNA was transformed into DH5α *Escherichia coli* competent cells, by heat shock at 42ºC for 90 seconds. The cells were incubated with 800 µl of SOC medium (from Q-Biogene) at 37ºC on a thermomixer (1000 rpm) for 1.5 hours, centrifuged in a Beckman Coulter Microfuge 18 centrifuge at about 2000xg for 3 minutes, re-suspended, and plated on LB agar (15 g agar/L LB broth, both from Fisher Scientific) with 100 µg/ml Kanamyacin. The plates were incubated at 37ºC for 16-18 hours.

Sequencing. Single colonies were re-streaked and grown in overnight culture with 30 µg/ml of Kanamyacin. The plasmid was purified from bacterial culture using the Pure Yield Plasmid Miniprep System, from Promega, according to the manufacturer's protocol. DNA

concentration was determined by Nanodrop scans at 260 and 280 nm. Plasmid was sequenced by GeneWiz, Inc using the universal T7 primer.

Introduction of the Second (E93R) Mutation. The plasmid obtained from the first mutation was used to introduce the second mutation. PCR-mutagenesis was carried out according to the protocol described previously, with the exception that the forward (5' GTC GAA GCG AAC CGC CGT GCC CTG GA 3') and reverse (5' CAG TTC TTC CAG GGC ACG GCG GTT CG 3') primers corresponding to the second mutation were used. The PCR product was transformed into BL21 *E. coli* competent cells; single colonies were re-streaked and DNA was purified and sequenced as described above.

Expression. BL21 *E. coli* cells expressing the target protein were inoculated in LB media with 30 μg/ml kanamyacin in a shaker at 180 rpm and 37°C [10]. The overnight culture was added to one liter of LB media with 30μg/ml of kanamyacin and grown in a shaker at 180 rpm and 37°C until it reached an O.D. of approximately 0.5 to 0.6 at 600 nm. At this point, isopropyl β-D-1-thiogalactopyranoside (IPTG) was added to a final concentration of 1 mM [10], in order to induce expression of the protein, and the culture was grown for an additional 4 hours. The cells were spun down by centrifugation for 15 minutes at 4000xg in 4°C. Pellets were collected and stored at - 80°C.

Protein Purification. The thawed pellet was suspended in lysate buffer (8 M urea, 100 mM NaH_2PO_4, 10 mM Tris, pH 8.0) and sonicated for 3 cycles of 5 minutes with 4 seconds of sonication and 6 second gaps or until the solution is clear. The lysate was centrifuged at 30,600xg for 45 minutes, filtered, and degassed by vacuum. Purification was conducted by a Nickel-NTA His Trap FF Column (from GE Healthcare) using the AKTA FPLC at room temperature under denaturing conditions [10]. Once the column and the FPLC were pre-washed

with sterile distilled water, the column was washed with approximately 15 column volumes of binding buffer (8 M urea, 100 mM NaH_2PO_4, 10 mM Tris, 20 mM imidazole, pH 8.0). The lysate was then loaded onto the column and the wash with binding buffer was continued for an additional few column volumes. The column washed with 15 column volumes of wash buffer 1 (8 M urea, 100 mM NaH_2PO_4, 20 mM Na citrate, 20 mM imidazole, pH 6.8, 15 column volumes of wash buffer 2 (8 M urea, 100 mM NaH_2PO_4, 20 mM Na citrate, 20 mM imidazole, pH 5.7), and 15 column volumes of wash buffer 3 (8 M urea, 100 mM NaH_2PO_4, 20 mM Na citrate, 20 mM imidazole, pH 4.7). The column was further washed by 15 column volumes of elution buffer 1 (8 M urea, 100 mM NaH_2PO_4, 10 mM Tris, 250 mM imidazole, pH 8.0), and then by 15 column volumes of elution buffer 2 (8 M urea, 100 mM NaH_2PO_4, 10 mM Tris, 500 mM imidazole, pH 8.0) [10]. All buffers were filtered and degassed. Purification was monitored by change in conductance and by absorbance at 280 nm.

SDS-PAGE. The purification fractions were analyzed using Mini Protean TGX pre-cast 10 well 12% SDS gels from Bio-Rad. The samples for the wells were prepared by adding Laemmli Sample Buffer (Bio-Rad) with β-mercaptoethanol to about 20 µl of each fraction, and heated at 95°C for about 4 minutes. The gels were run for 30 to 45 minutes at 120 V and stained using Coomassie Simply Blue SafeStain acquired from Invitrogen.

Quick Refolding. Dynamic Light Scattering (DLS) was performed in different buffers at 1:20 fold dilutions from the elution fractions that demonstrated the highest protein concentration. Refolding in each buffer was achieved by diluting 50 µl of elution sample into 950 µl of buffer and spinning for approximately 15 to 20 minutes. DLS was done on a Zetasizer Nano S instrument (Malvern) with a 633 nm He-Ne laser [8]. The six buffers were: 1) 20 mM Tris, 40 mM NaCl, 5% glycerol, pH 8.5, 2) 20 mM Tris, 150 mM NaCl, 5% glycerol, pH 8.5, 3) 20 mM

Hepes, 40 mM NaCl, 5% glycerol, pH 7.5, 4) 20 mM Hepes, 150 mM NaCl, 5%, glycerol pH 7.5, 5) 20 mM Mes, 40 mM NaCl, 5% glycerol, pH 6.5, and 6) 20 mM Mes, 150 mM NaCl, 5% glycerol, pH 6.5 [5]. This provides a final urea concentration of 0.4 M. The measurements were taken at room temperature.

Dialysis. The fractions with the greatest absorbance that also demonstrated the presence of protein at the correct band on the gels were pooled and dialyzed in 1 liter of the optimal buffer determined by quick refolding. A dialysis bag with a pore size of 8 kDa was used and dialysis was carried out over a period of 24 hours, with a replacement of 1 liter of buffer after approximately 12 hours. The protein was stored at -80°C in aliquots.

Concentration Determination. Nanodrop and BCA protein assay were used to determine the concentration of the pooled elution fractions. With the Nanodrop, absorbance of the sample was measured at 280 nm and concentration in mg/ml was calculated using the extinction coefficient and molecular weight of the protein. The BCA protein assay was performed according to the standard protocol of the BCA Protein Assay kit from ThermoScientific. Absorbance measurements were taken at 620 nm on a plate reader and concentration was determined by use of the graphed standard curve.

Direct Refolding. Aliquots of the protein samples were dialyzed in 20 fold dilutions of each of the six buffers described above: 1) 20 mM Tris, 40 mM NaCl, 5% glycerol, pH 8.5, 2) 20 mM Tris, 150 mM NaCl, 5% glycerol, pH 8.5, 3) 20 mM Hepes, 40 mM NaCl, 5% glycerol, pH 7.5, 4) 20 mM Hepes, 150 mM NaCl, 5%, glycerol pH 7.5, 5) 20 mM Mes, 40 mM NaCl, 5% glycerol, pH 6.5, and 6) 20 mM Mes, 150 mM NaCl, 5% glycerol, pH 6.5 [5]. These samples had 0 M concentration of urea. Refolding was conducted using the same methods described above

and sample was analyzed with DLS at room temperature using the same instrument described previously.

Stability Tests. The dialyzed protein was refolded into the four most optimal buffers and 7 aliquots of 500 µl of sample in each buffer were stored at 4°C for one month's time [10]. Furthermore, dialyzed stock protein in the optimal buffer was placed at room temperature and at 4°C for one month. DLS measurements were taken, under the same condition described above, for each experimental set up at days 0, 1, 7, 14, 21, and 28.

Transmission Electron Microscopy. Refolded protein samples were placed on a FCF400 Copper Formvar Carbon Film (Electron Microscopy Sciences, Inc) Grid that was charged using a Harrick Plasma Cleaner PDC-32G. The grid with sample was then stained with 1% uranyl acetate and washed with distilled water (negative staining). The sample was imaged with a FEI Tecnai T12 S/TEM [8].

Results

Protein Purification. Pandora F5de, the target protein, was purified using a Ni-NTA column, since it contains a histidine tag. The column was washed with a pH gradient in order to remove other proteins, impurities, and contaminants, such as nonspecifically binding molecules, from the column. The protein eluted in 250 mM imidazole, as expected, in fractions 22 through 31, as evidenced by the large absorbance peak in this range (figure 4). Imidazole competed with the histidines of the protein for binding with the nickel-bound beads, allowing the protein to fall off the column. The large absorbance peak in fractions 1 and 2 indicated that the flow of protein through the column once it was directly loaded. Progress of the purification and the equilibration of the column with each buffer were monitored by change in conductance, as indicated by the brown graph in figure 1. The SDS-PAGE gels (figure 5) demonstrated the presence of Pandora F5de as the large band of protein at about 20 kDa in the lysate, flow through, and eluted fractions 22 through 31. Additionally, in the early fractions with washes at different pH levels, there was evidence of elution of contaminant proteins. The gels indicated that the eluted target protein was very pure, as there was no significant presence of other contaminants with one little exception: The very faint band between 30 and 40 kDa could either be another protein from the bacteria that contains exposed histidines or, more than likely, it was a dimer of the target protein. Given that this band was predominantly in the sample with the greatest concentration of target protein, it is likely that there was some dimerization. However, this is a matter that ought to be explored in further studies, and will not be further dealt with here. Given the significant presence F5de in the flow through, a larger column might have resulted in an even greater yield of protein. However, for the purposes of these preliminary studies of the construct, the amount of purified protein obtained was sufficient.

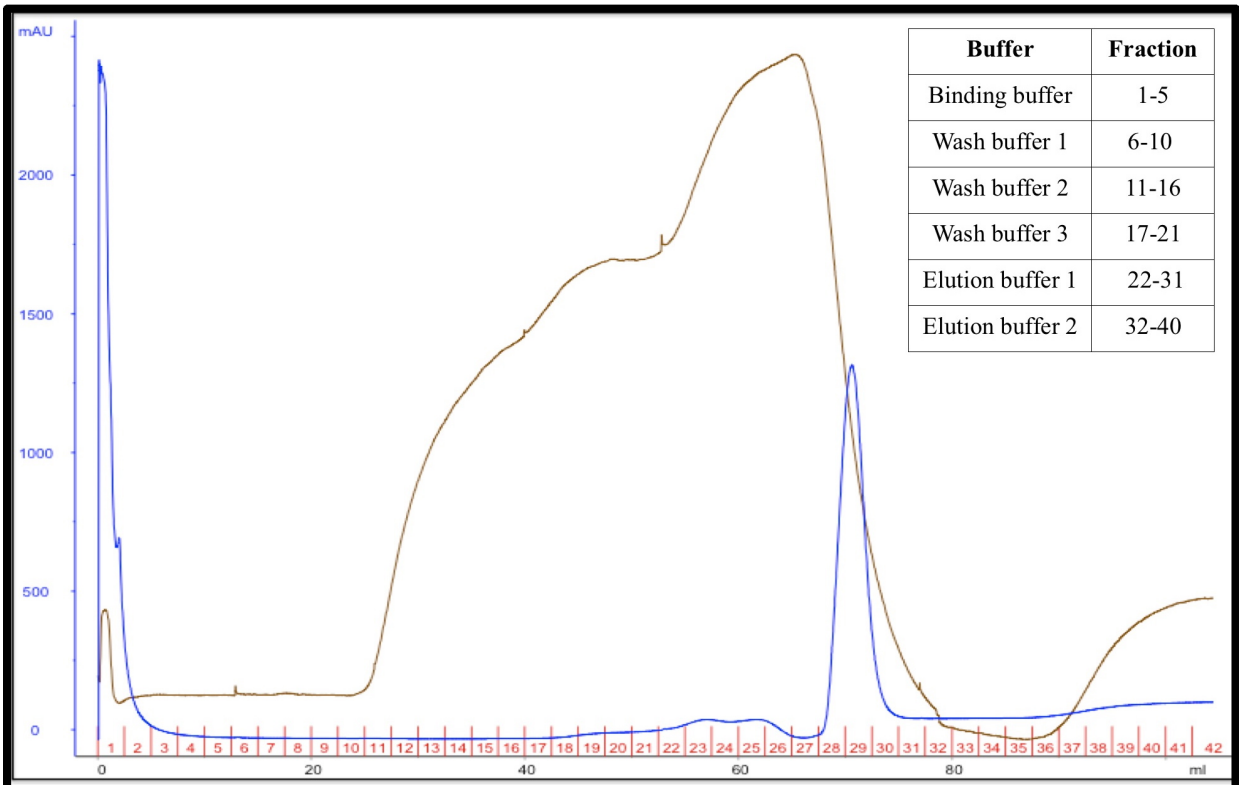

Buffer	Fraction
Binding buffer	1-5
Wash buffer 1	6-10
Wash buffer 2	11-16
Wash buffer 3	17-21
Elution buffer 1	22-31
Elution buffer 2	32-40

Figure 4. Purification Profile in absorbance units versus elution volume. In red is shown the fraction number, each of which is 2.5 ml. The blue graph charts the absorbance at 280 nm and the brown graph charts conductivity. The upper right hand corner describes at which fraction each buffer was added to the column.

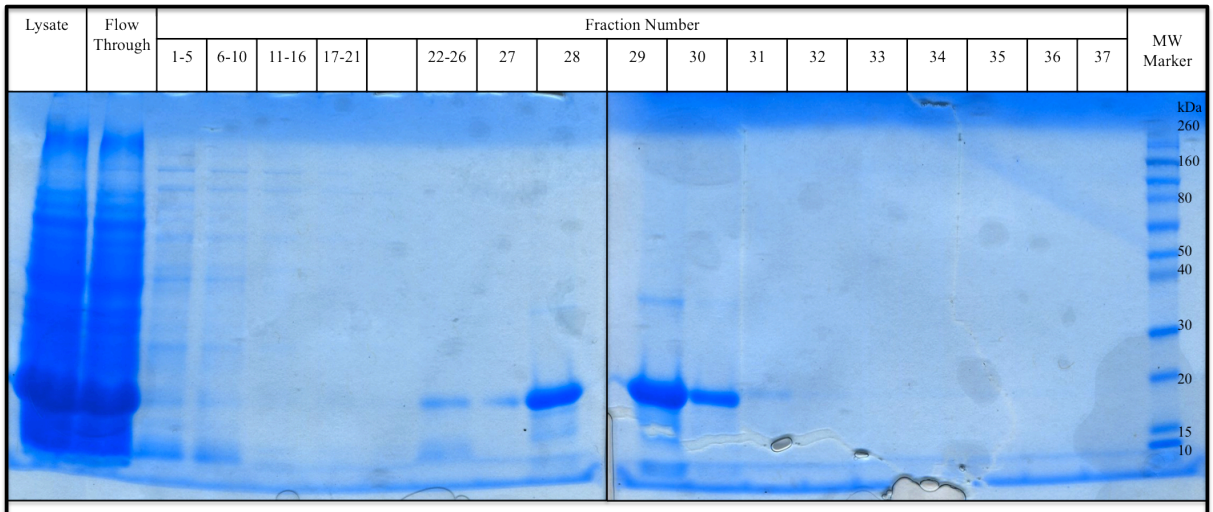

Figure 5. Fraction Contents. Two 10 well 12% SDS gels run with fraction samples indicating the presence of the target protein at band with an approximate molecular weight of 20 kDa in fractions 28-30. The lysate and flow through indicate presence of target protein as well.

Quick-Refolding. Since the purification was conducted under denaturing conditions, it was essential to determine an appropriate buffer to dialyze the protein. Samples from fraction 29,

which had the highest absorbance peak (figure 4) and thickest band (figure 5), were tested under six different refolding conditions. These conditions were tested because previous experience with these constructs has shown that refolding can usually be achieved in one of the conditions. Since significantly high concentrations of imidazole (250 mM) and urea (8 M) were present in the sample from the purification, it was important to make dilutions (in this case 1:20) of the sample into each buffer to determine the best buffer for refolding and storage. The dilutions resulted in an approximate concentration of imidazole and urea at, 80 mM and 400 mM respectively. Several scans from dynamic light scattering were used to indicate the approximate diameter of each protein and to detect self-assembly and/or aggregation. The optimal buffer for refolding was clearly 20 mM Tris with 40 mM NaCl at a pH of 8.5 (T40 buffer), as it resulted in the most uniform distribution of particles and essentially no aggregation (figure 6E). In Mes, F5de exhibited a great deal of aggregation, regardless of the salt concentration. In Hepes there was far less aggregation than in Mes; however, it was not at all comparable to the distribution of nanoparticles in Tris buffer. The diameter of the protein in T40 buffer was determined to be 22.03 nm, which was close to the expected value of about 25 nm. This indicated that the protein was properly assembled into a symmetrical self-assembling structure, as expected. However, since the diameter was slightly smaller, it is possible that the structure formed least common multiple (LCM) units with 15 protein chains per particle, rather than the complete icosahedral with 60 protein chains per particle. This would have to be determined by TEM. While there was some aggregation in T40, which could be attributed to any number of factors, not least of which the presence of imidazole and urea, the significant presence of assembled particle of this diameter clearly indicated that 20 mM Tris, 40 mM NaCl, pH of 8.5 was the best buffer to use for dialysis.

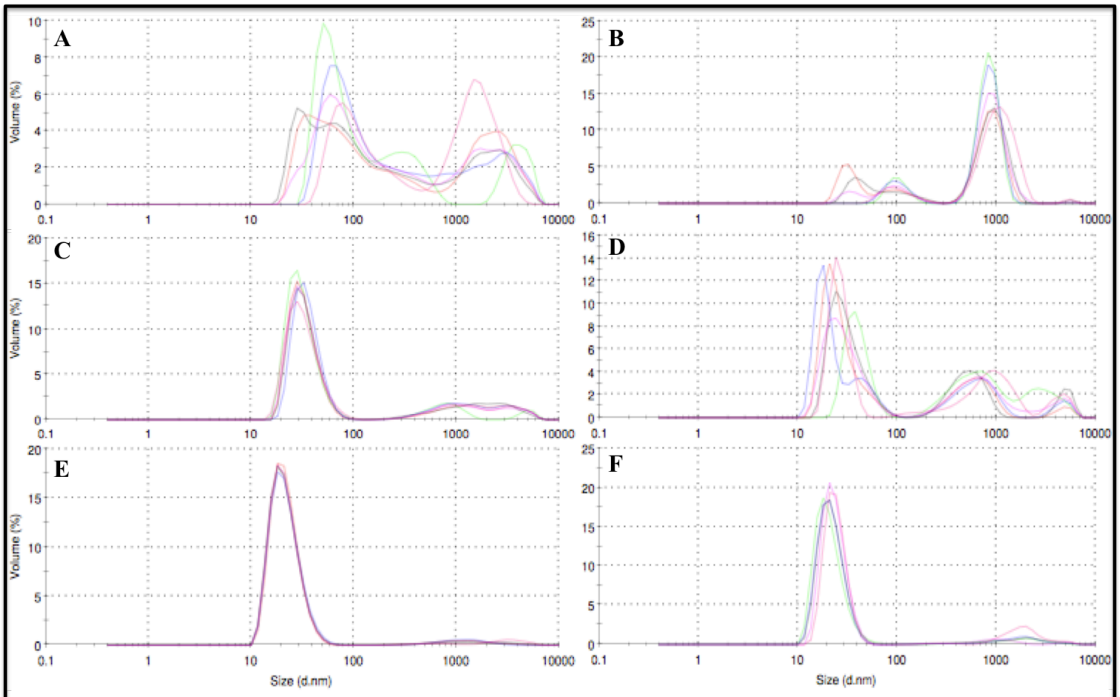

Figure 6. Quick Refolding. Target protein in fraction 29 was refolded, directly upon purification, in 1 to 20 dilutions in each buffer. Five scans of each sample in different buffers are shown in each graph: A) 20 mM Mes, 40 mM NaCl, pH 6.5, B) 20 mM Mes, 150 mM NaCl, pH 6.5, C) 20 mM Hepes, 40 mM NaCl, pH 7.5, D) 20 mM Hepes, 150 mM NaCl, pH 7.5, E) 20 mM Tris, 40 mM NaCl, pH 8.5, F) 20 mM Tris, 150 mM NaCl, pH 8.5.

Dialysis and Protein Concentration. Fractions 28, 29, and 30 were pooled, as they contained the largest absorbance peaks and bands of the target protein, and dialyzed against one liter of T40 buffer twice over a period of 24 hours. In this case, imidazole, urea, and other elution buffer 1 components were diluted at least 10,000-fold, resulting in 8 mM urea and 0.25 mM imidazole, which is essentially negligible compared to their previous concentrations. The pooled and dialyzed protein concentration was determined to be 0.46 mg/ml by BCA Assay (figure 7A,B) and 0.58 mg/ml by absorbance scans with a Nanodrop spectrophotometer (figure 7B). Given that the assays measure two different components related to protein structure and thereby can be used to determine concentration, the discrepancy between the concentrations is not necessarily surprising. The difference in concentration in this case, however, is not critical as this information was only used to approximate the concentration of protein tested for direct refolding and for electron microscopy.

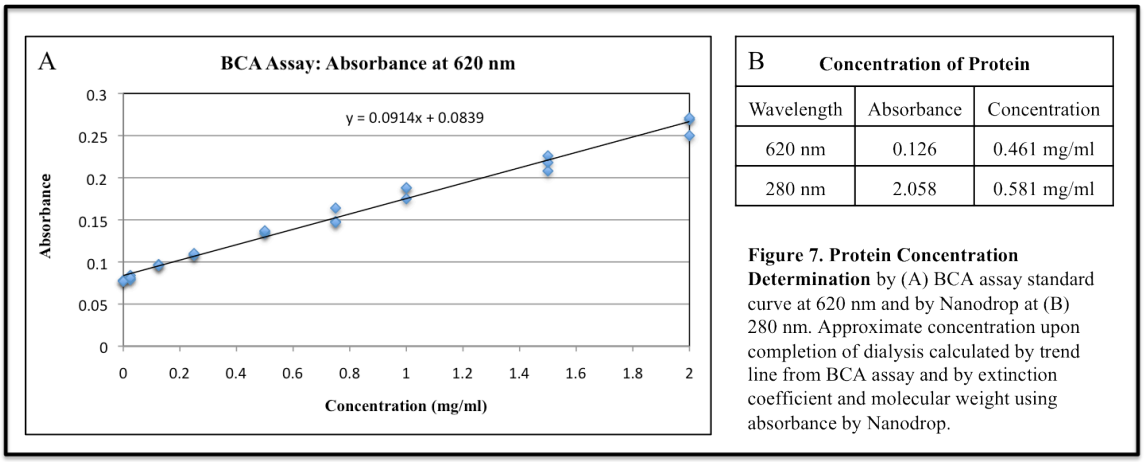

B **Concentration of Protein**

Wavelength	Absorbance	Concentration
620 nm	0.126	0.461 mg/ml
280 nm	2.058	0.581 mg/ml

Figure 7. Protein Concentration Determination by (A) BCA assay standard curve at 620 nm and by Nanodrop at (B) 280 nm. Approximate concentration upon completion of dialysis calculated by trend line from BCA assay and by extinction coefficient and molecular weight using absorbance by Nanodrop.

Direct Refolding. The pooled F5de in T40 buffer was dialyzed into each of the different buffers and measurements were taken by DLS, which demonstrated that Tris buffer, whether at 40 mM or 150 mM NaCl, still remained the optimal buffer. While the Hepes buffer at low concentrations of salt exhibited some aggregation and a lack of uniform protein assembly, Hepes at high salt concentration did produce a uniform and properly assembled structure (figure 8C, D). The diameter of the protein in 20 mM Hepes, 150 mM NaCl, pH 7.5 (H150 buffer) was found to be 21.36 nanometers. In the Tris buffers, which seem to result in no aggregation and exhibit a nearly uniform distribution of particles, demonstrated a nanoparticle diameter of 18.17 nm in T40 buffer and 20.74 nm in T150 buffer. The slightly greater diameter in both buffers with higher salt concentration might be due to the fact that high levels of salt can increase hydrophobic molecular interactions and thus, either species with more protein chains per assembly unit were formed (i.e. icosahedral particles versus LCM units) or particles started to slightly stick together, as can be seen in the exceptional difference in particle distribution between Mes buffer with 40 mM NaCl versus Mes with 150 mM NaCl (figure 8A, B) and especially in Hepes with 40 mM NaCl versus 150 mM NaCl. However, this is a matter to be explored in further studies that reach beyond the scope of these experiments.

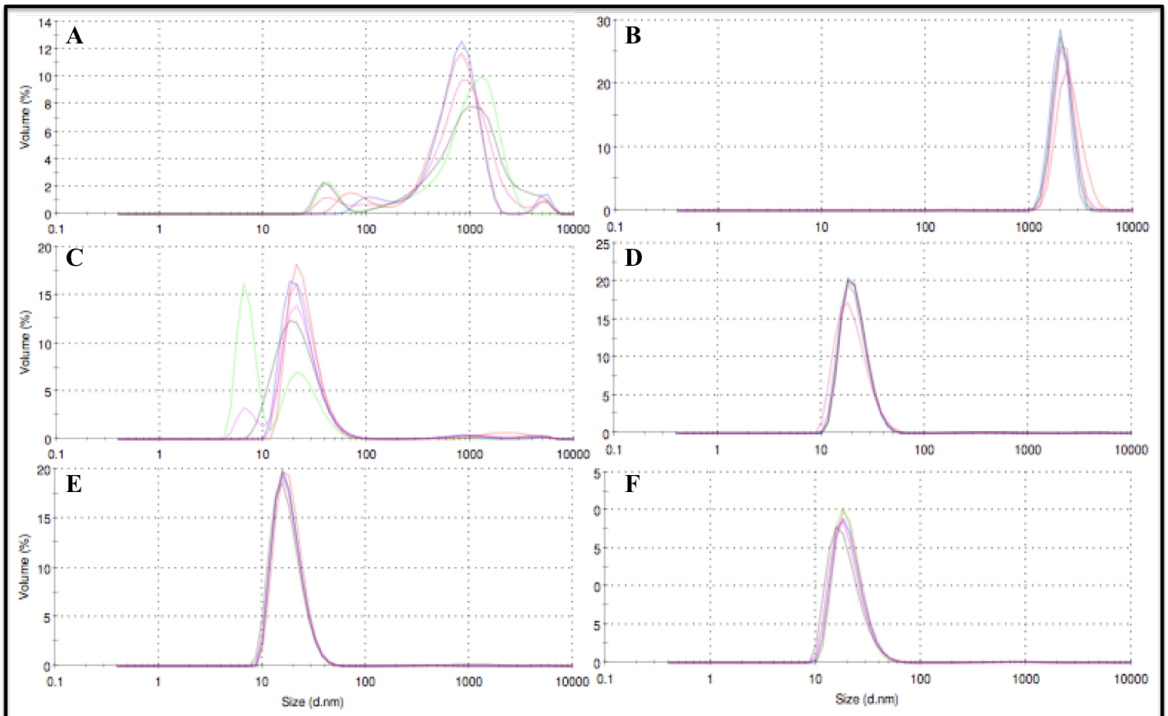

Figure 8. Direct Refolding. Target protein was dialyzed in optimal buffer then and refolded, in 1 to 20 dilutions in each buffer. Five scans of each sample in different buffers are shown in each graph: A) 20 mM Mes, 40 mM NaCl, pH 6.5, B) 20 mM Mes, 150 mM NaCl, pH 6.5, C) 20 mM Hepes, 40 mM NaCl, pH 7.5, D) 20 mM Hepes, 150 mM NaCl, pH 7.5, E) 20 mM Tris, 40 mM NaCl, pH 8.5, F) 20 mM Tris, 150 mM NaCl, pH 8.5.

Stability Tests. The stability of the F5de nanoparticle construct was studied over the period of one month (28 days). The purified protein that was already refolded in four different buffers (H40, H150, T40, and T150) was measured by DLS once a week and stored at 4ºC. Additionally, a sample of the nanoparticle in T40 buffer was placed at room temperature and at 4ºC and measurements were taken by DLS. The particles were overall very stable, as is evident in figures 9, 10, and 11. In Hepes buffers, with some aggregation from the outset, it seemed that there were measurable increases in aggregation of the protein over the course of one month. Also, the assembled nanoparticle diameter exhibited significant increases in diameter, especially in Hepes with the high salt concentration. The initial diameter of 20.0 nm more than doubled to 46.1 nm by the end of the month, and by day 7, the diameter was already 10 nm greater in diameter than initially. This clearly indicates that aggregation occurred over time. In 20 mM Hepes and 40 mM NaCl, however, over the course of the month the nanoparticle diameters were

19.9 nm on day 1, 23.69 nm on day 7, 24.46 nm on day 14, 24.46 nm on day 21, and 25.65 nm on day 28. While the diameters were closer to the expected icosahedral nanoparticle diameter of 25 nm, the particles were not as uniform in distribution over the course of the month as in Tris (figure 10). In the two Tris buffers, shown in figure 10, the nanoparticles appeared to be far more uniformly distributed in solution. As the month progressed there was essentially no aggregation over time. In 20 mM Tris with 40 mM NaCl, the initial diameter of 16.97 nm, was followed by diameters of 23.03 nm on day 7, 19.76 nm on day 14, 15.94 nm from day 21, and 15.81 nm on day 28. Just as in quick refolding (figure 6) and direct refolding (figure 8), Tris with 40 mM NaCl appeared to be the buffer in which the nanoparticles were most uniformly assembled. However, even though this was the case, these measured diameters were smaller than would be expected for a fully assembled icosahedral nanoparticle, which might affect the immunogenicity of the nanoparticles, since, in general, immunogenicity decreases for particles with a diameter smaller than 20 nm. Tris with 150 mM NaCl seemed to result in less aggregation (figure 10A, B) than any of the other buffers. Furthermore, in 20 mM Tris and 150 mM NaCl buffer the nanoparticles exhibited the least variation in the hydrodynamic diameter, with 19.26 nm on day 1, 22.86 nm on day 7, 19.78 nm on day 14, 19.78 nm on day 21, and 19.44 nm on day 28. Additionally, measurements taken over the course of a month in 20 mM Tris and 40 mM NaCl from samples stored at 4ºC and room temperature indicate that there is essentially no difference in the distribution of the nanoparticle sizes between the two temperatures (figure 11). Overall, these tests demonstrate that the construct was exceptionally stable in Tris buffer, whether stored at 4ºC or at room temperature. In both cases, the diameter of the nanoparticles throughout the month was about 18 nm, indicating that the assembled nanoparticle maintained its shape and stability for one month in both conditions.

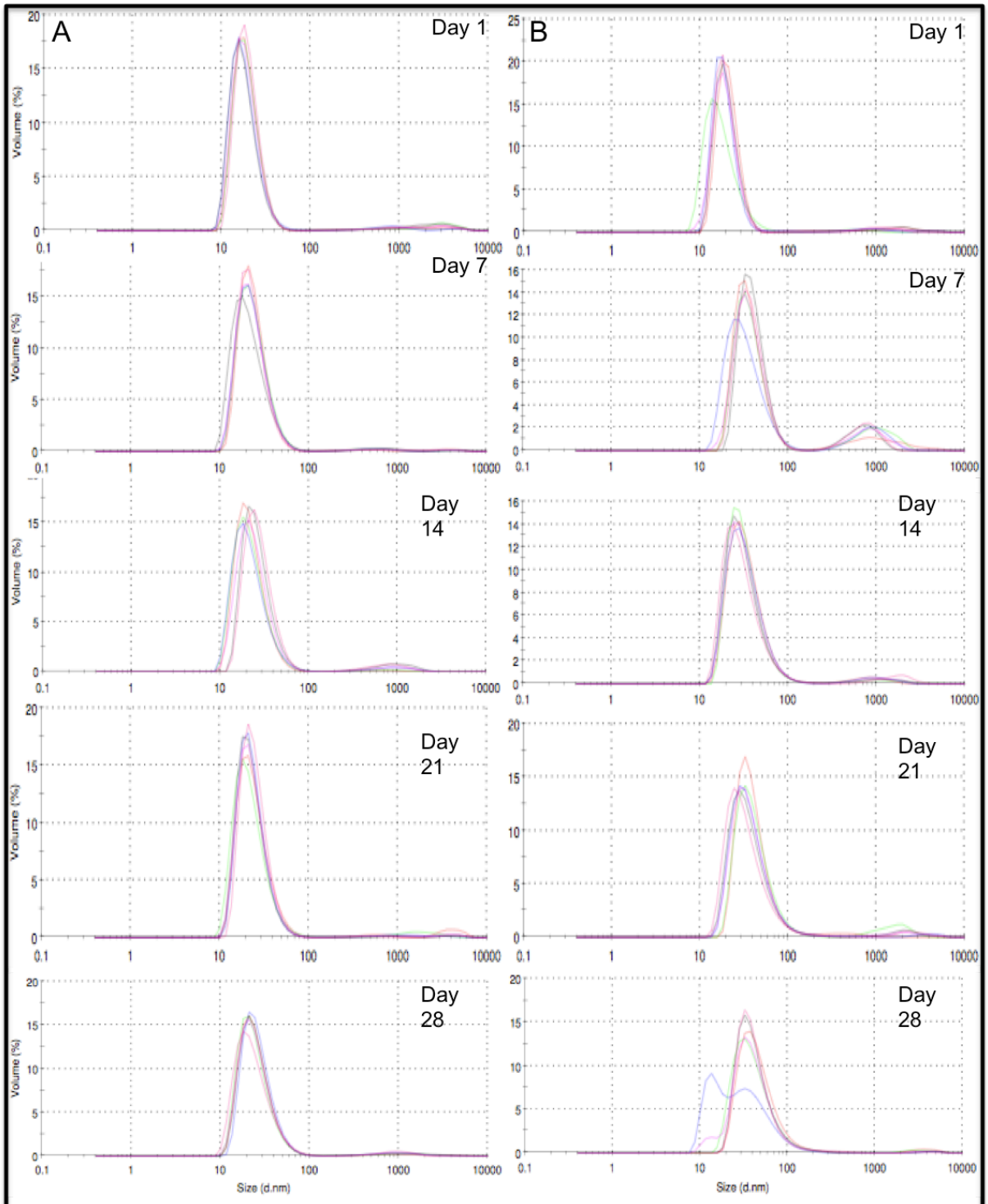

Figure 9. Stability Testing in Hepes Buffer. DLS measurements were taken once a week over the period of a month of the pooled and dialyzed protein in (A) 20 mM Hepes, 40 mM NaCl, pH 7.5 and (B) 20 mM Hepes, 150 mM NaCl, pH 7.5.

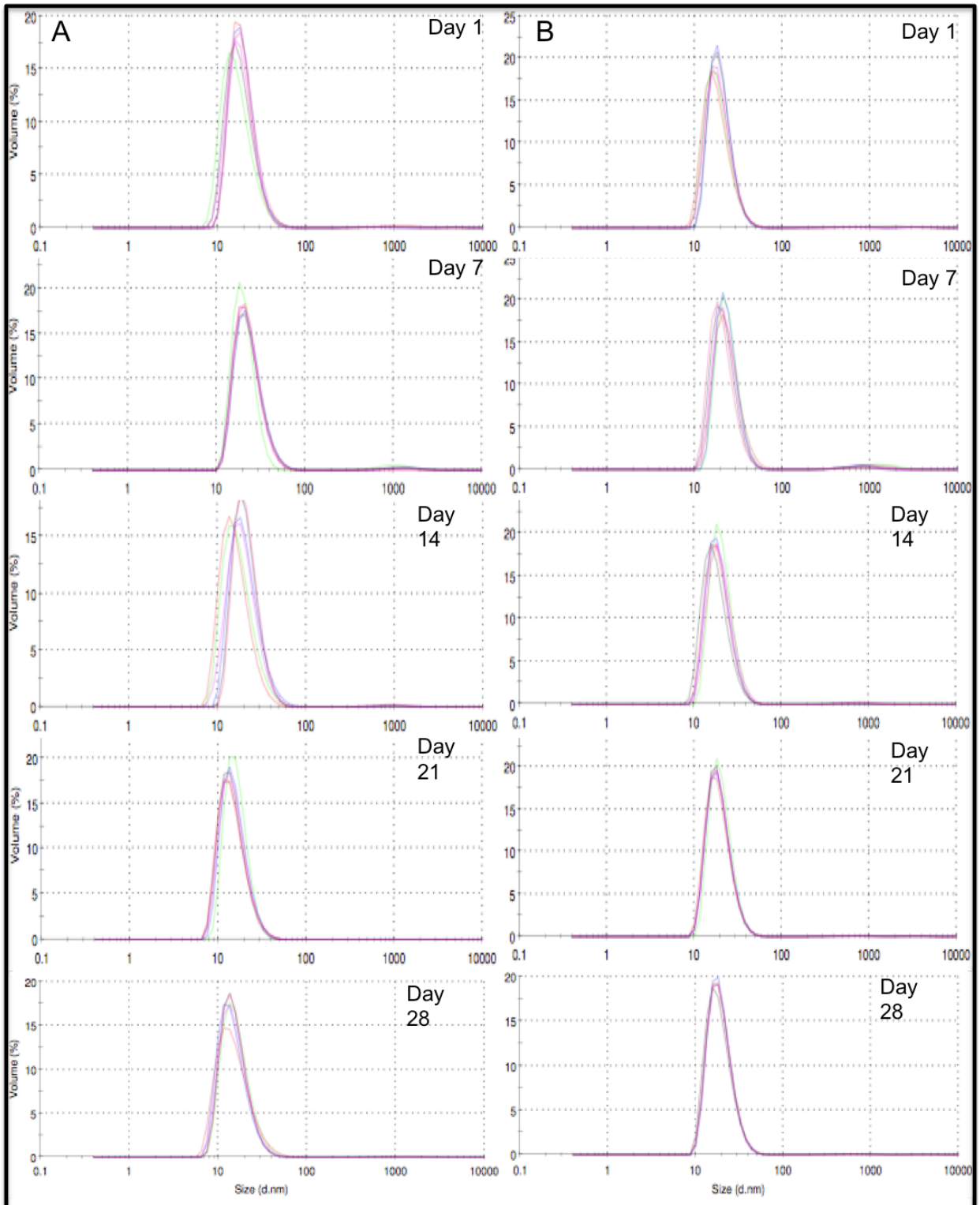

Figure 10. Stability Testing in Tris Buffer. DLS measurements were taken once a week over the period of a month of the pooled and dialyzed protein in (A) 20 mM Tris, 40 mM NaCl, pH 8.5 and (B) 20 mM Tris, 150 mM NaCl, pH 8.5.

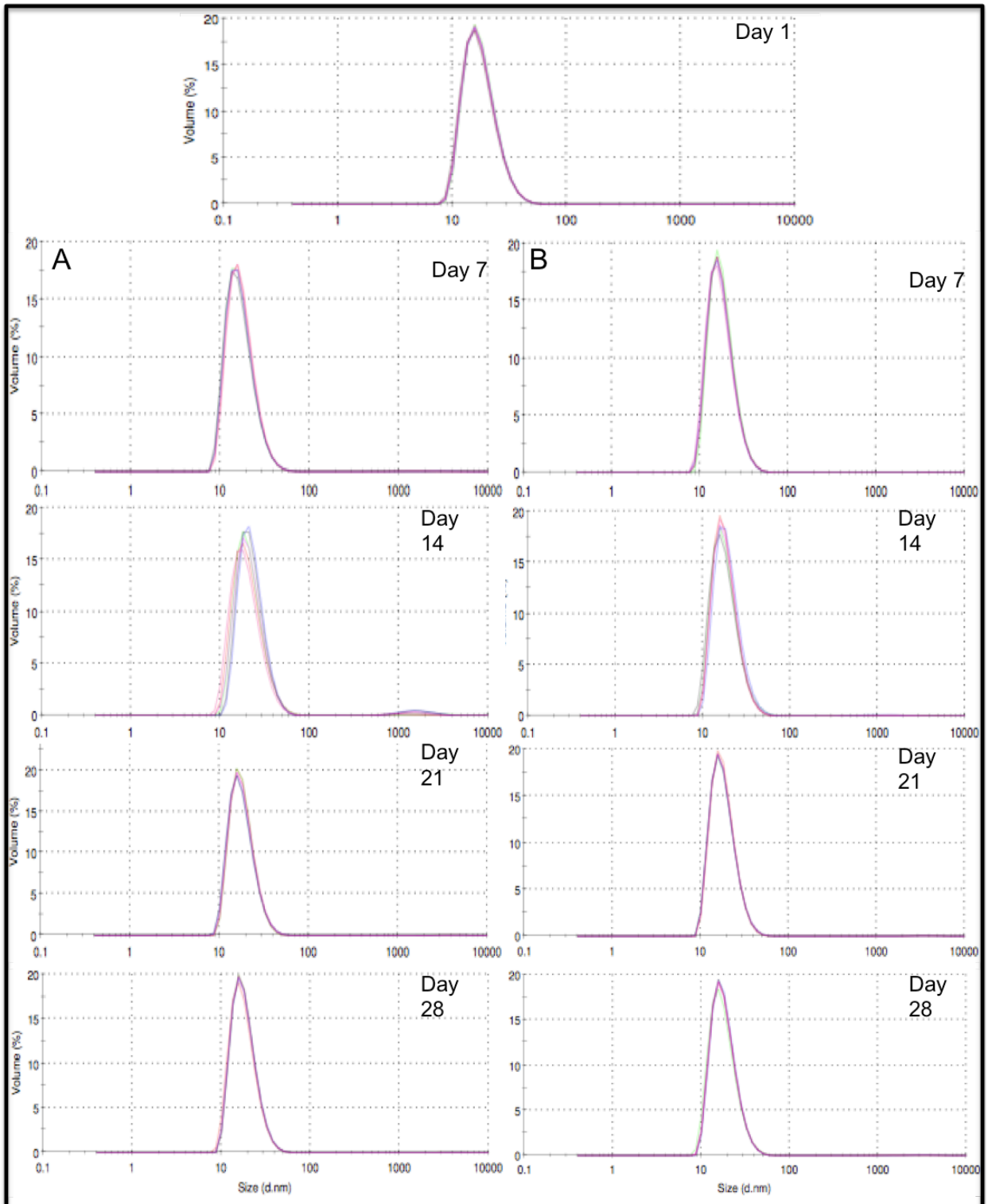

Figure 11. Stability Testing at Different Temperatures in Tris Buffer. DLS measurements were taken once a week over the period of a month of the pooled and dialyzed protein in (A) 20 mM Tris, 40 mM NaCl, pH 8.5, stored at 4°C and (B) 20 mM Tris, 40 mM NaCl, pH 8.5, and stored at room temperature.

Transmission Electron Microscopy. Images of Pandora F5de were taken, at 120,000x magnification, immediately upon refolding in 20 mM Tris, 40 mM NaCl, and pH 8.5 and then after one month in the same buffer and in 20 mM Hepes, 40 mM NaCl, pH 7.5. The images in Tris indicated the nearly uniform presence of partially assembled nanoparticles and appear to be so-called LCM units with 15 protein chains per nanoparticle with some indications of slightly larger more globular species, which would likely be a fully assembled icosahedral nanoparticle (figure 12). This correlated with the DLS direct refolding data of smaller than expected nanoparticle diameters discussed previously. Additionally, there were some white rod-like structures in the images, which could have been contaminants in the buffer, the copper grid, or in the uranyl acetate as these structures were also visible on EM grid preparations without protein. The images from day one (figure 12A) showed more discrete individual particles, while the images taken after one month (figure 12b) demonstrated closer association between particles due to a higher protein concentration. Overall, though, the particle size and distribution was very similar between the two, just as in DLS. The disparity in crispness between the two images was likely due to differences in preparation and staining of the two grids. The image taken of F5de in 20 mM Hepes and 40 mM NaCl (figure 13) after one month indicated the presence of a more heterogeneous species than was found in the images at pH 8.5. For the most part, the larger sized particles appeared to be smaller sized particles associating, rather than formations of the icosahedral nanoparticles, thus confirming the presence of LCM units. In Hepes, just as indicated by the DLS, there was a far less homogeneous distribution and the indication of a nanoparticle diameter closer to 25 nm, the expectation for the icosahedral species, was likely due to the clumping of the smaller species over the course of one month, rather than formation of the fully assembled nanoparticles.

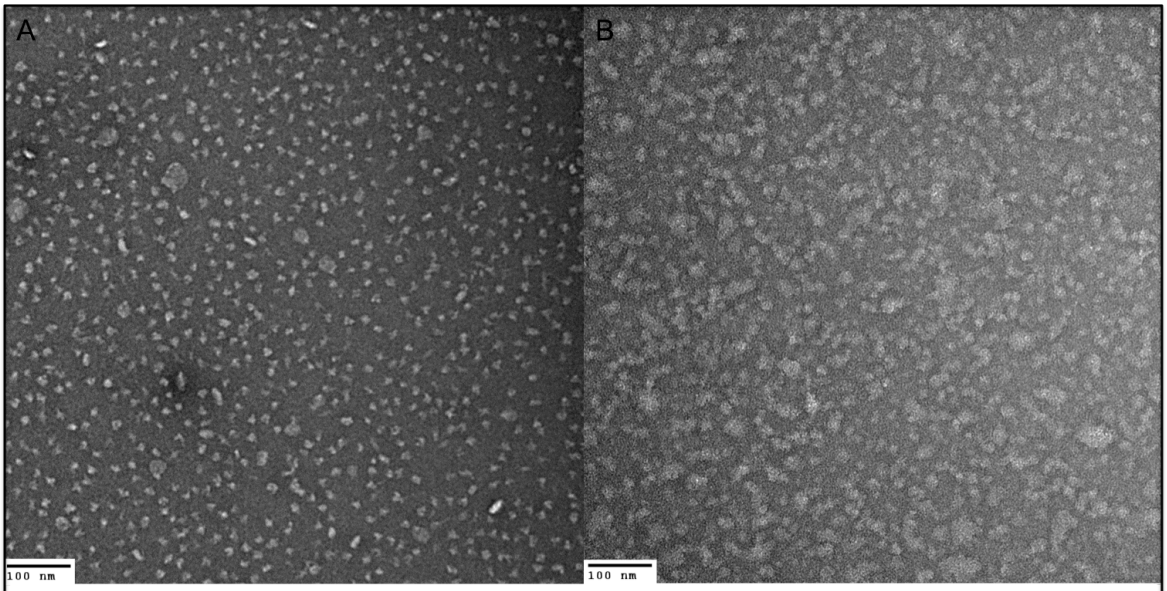

Figure 12. TEM Images of Pandora F5de in Tris Buffers. Pandora F5de was refolded in 20 mM Tris, 40 mM NaCl, and pH 8.5 and images were taken at 120000x magnification on A) Day 1 and B) Day 28.

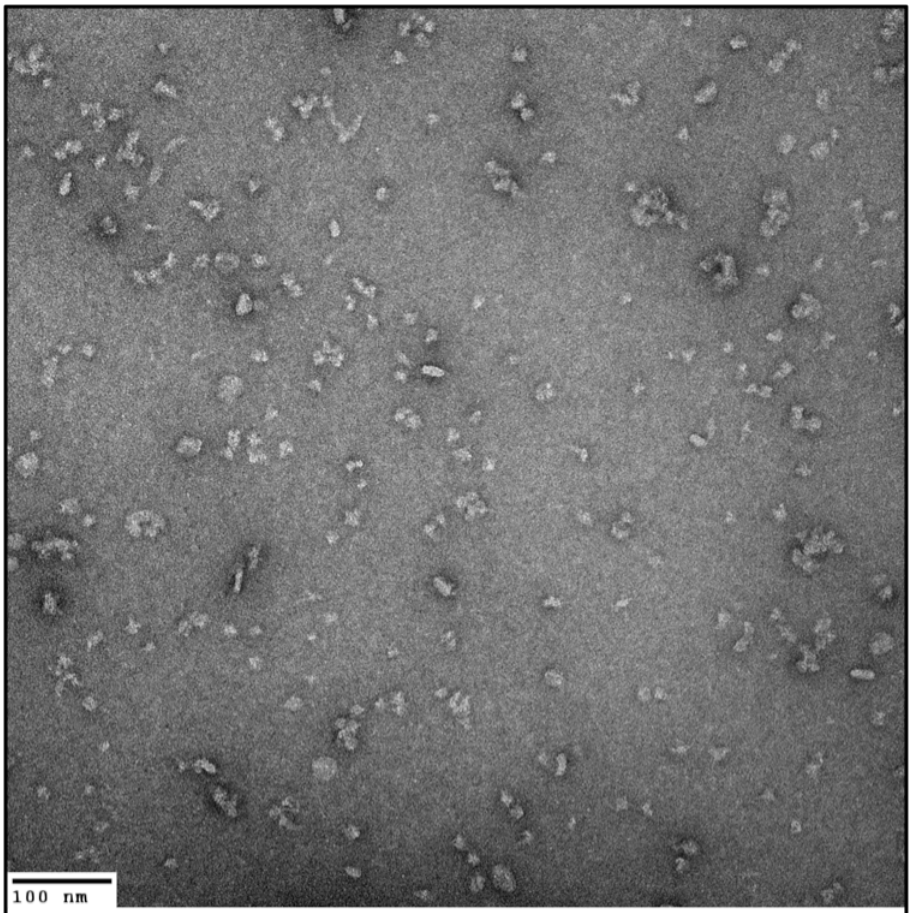

Figure 13. Pandora F5de in Hepes Buffer. Protein refolded in 20 mM Hepes, 40 mM NaCl, pH 7.5 and TEM image taken at 120000x magnification after 28 days.

Discussion

According to the DLS and TEM data of the purified Pandora F5de construct, the protein did self-assemble, but they did not form the complete icosahedrally symmetrical 60-mer nanoparticle. Given that the hydrodynamic radius was approximately 20 nm or slightly smaller and was uniformly distributed in solution, it can be inferred that the nanoparticles formed so-called LCM units with 15 protein chains per nanoparticle. The diameters of the nanoparticles measured by DLS were slightly smaller than expected, sometimes around 16 to 18 nm, especially in 20 mM Tris with 40 mM NaCl buffer. This smaller diameter could have been a direct result of the switch in the charges (glutamic acid and arginine) in the backbone of the construct between the negative pentamer and the more positive trimer, resulting in a more soluble and less hydrophobic protein chain. The protein refolded exceptionally well in Tris buffer, both at high and low salt concentrations and maintained its shape and uniformity, both according to DLS and TEM, in solution for at least one month, both at 4°C and room temperature with no signs of aggregation. The protein nanoparticle was evidently stable, which is an extremely important consideration for vaccine development. However, since the nanoparticle size was smaller than expected and the fully formed icosahedral species was not predominantly present in solution, further studies will have to be performed in order to determine the immunogenicity of this construct in its optimal refolding buffer.

The fact that the nanoparticles were uniform and stable, even if not a fully formed icosahedral species, was very promising for using this construct and similar ones with this basic design in malaria vaccine development. Given the similarity between this construct and PfCSP-KMY-SAPN, which was discussed previously, it would likely exhibit the similar high levels of immunity *in vivo* [8]. Furthermore, given the fact that in both cases $CD8^+$ T-cell, B-cell, and

$CD4^+$ helper T-cell epitopes were incorporated into the nanoparticle constructs, F5de shares similar potential for further development. For this to be the case, it would be necessary to further purify the protein, using perhaps ion exchange chromatography and gel filtration, as has been done previously when preparing a protein for *in vivo* studies [10]. Additionally, definitively resolving the nature of the species that eluted, at very low concentration, with Pandora F5de would be important. Also, a modification to the purification protocol that might have prevented the elution of the species of about double the molecular weight of the target protein might have been to elute with a linear gradient of imidazole, rather than directly with a concentration where the protein was expected to elute. This would have allowed other potentially contaminating proteins to elute earlier. As this construct was shown to be most stable at a relatively high pH compared to physiological conditions, there might also be further interest in determining if the construct can be refolded closer to a pH of 7, even though there were initial difficulties with 20 mM Hepes buffers at a pH of 7.5, by testing different excipients (such as e.g. trehalose or sucrose) during refolding or testing conditions with even lower salt concentrations. These potential modifications would most definitely be relevant to further studies of this construct, but also for future analyses of these self-assembling peptide nanoparticle malaria vaccine prototypes.

References

1. WHO. World malaria report. 2012. http://www.who.int (last accessed 06 March 2013).

2. Agnandji ST, et al.; RTS,S Clinical Trials Partnership (2011) First results of phase 3 trial of RTS,S/AS01 malaria vaccine in African children. N Engl J Med 365:1863–1875.

3. Wahome N, Pfeiffer T, Ambiel I, Yang Y, Keppler OT, Bosch V, Burkhard P. 2012. Conformation-specific display of 4E10 and 2F5 epitopes on self-assembling protein nanoparticles as a potential HIV vaccine. Chem. Biol. Drug Des. 80, 349–357 (doi:10.1111/j.1747-0285.2012.01423.x) doi: 10.1111/j.1747-0285.2012.01423.x.

4. Pimentel TA, Yan Z, Jeffers SA, Holmes KV, Hodges RS, Burkhard P. 2009. Peptide nanoparticles as novel immunogens: design and analysis of a prototypic severe acute respiratory syndrome vaccine. Chem. Biol. Drug Des. 73, 53–61 (doi:10.1111/j.1747-0285.2008.00746.x) doi: 10.1111/j.1747-0285.2008.00746.x.

5. Raman S, Machaidze G, Lustig A, Olivieri V, Aebi U, Burkhard P. 2009. Design of peptide nanoparticles using simple protein oligomerization domains. Open Nanomed. J. 2, 15–26 (doi:10.2174/1875933500902010015) doi: 10.2174/1875933500902010015.

6. Raman S, Machaidze G, Lustig A, Aebi U, Burkhard P. 2006. Structure-based design of peptides that self-assemble into regular polyhedral nanoparticles. Nanomed. Nanotechnol. Biol. Med. 2, 95–102 (doi:10.1016/j.nano.2006.04.007) doi: 10.1016/j.nano.2006.04.007.

7. Doll TAPF, Raman S, Dey R, Burkhard P. 2013 Nanoscale assemblies and their biomedical applications. J R Soc Interface10: 20120740. http://dx.doi.org/10.1098/rsif.2012.0740.

8. Kaba SA, McCoy ME, Doll TAPF, Brando C, Guo Q, et al. (2012) Protective Antibody and CD8+ T-Cell Responses to the Plasmodium falciparum Circumsporozoite Protein Induced by a Nanoparticle Vaccine. PLoS ONE 7(10): e48304. doi:10.1371/journal.pone.0048304.

9. Doud MB, Koksal AC, Mi LZ, Song G, Lu C, and Springer TA. Unexpected fold in the circumsporozoite protein target of malaria vaccines. Proc Natl Acad Sci U S A. 2012 May 15; 109(20): 7817–7822.

10. Q. Guo, D. Dasgupta, T.A.P. Doll, P. Burkhard, D.E. Lanar, Expression, purification and refolding of a self-assembling protein nanoparticle (SAPN) malaria vaccine, Methods (2013), doi: http://dx.doi.org/10.1016/j.ymeth.2013.03.025.